Available online at www.sciencedirect.com
ScienceDirect
Developmental Biology 302 (2007) 218–229
DEVELOPMENTAL BIOLOGY
www.elsevier.com/locate/ydbio

Foxe3 is required for morphogenesis and differentiation of the anterior segment of the eye and is sensitive to *Pax6* gene dosage

Åsa Blixt [a], Henrik Landgren [a], Bengt R. Johansson [b], Peter Carlsson [a,*]

[a] *Dept. of Cell and Molecular Biology, Göteborg University, Box 462, 405 30 Göteborg, Sweden*
[b] *The Electron Microscopy Unit, Dept. of Anatomy and Cell Biology, Göteborg University, Göteborg, Sweden*

Received for publication 12 June 2006; revised 8 September 2006; accepted 11 September 2006
Available online 16 September 2006

Abstract

The *dysgenetic lens* (*dyl*) mouse mutant has mutations in *Foxe3*, which inactivate DNA binding by the encoded forkhead transcription factor. Here we confirm, by targeted inactivation, that *Foxe3* mutations are responsible for the *dyl* phenotype, which include loss of lens epithelium; a small, cataractic lens; and failure of the lens to detach from the surface ectoderm. In contrast to a recent report of targeted *Foxe3*, we found no phenotypic difference between *dyl* and $Foxe3^{-/-}$ mutants when congenic strains were compared, and thus nothing that argues against $Foxe3^{dyl}$ being a null allele. In addition to the lens, most tissues of the anterior segment–iris, cornea, ciliary body and trabecular meshwork–are malformed or show differentiation defects. Many of these abnormalities, such as irido-corneal and irido-lenticular adherences, are present in a less severe form in mice heterozygous for the *Foxe3* mutation, in spite of these having an intact lens epithelium. Early *Foxe3* expression is highly sensitive to a halved *Pax6* gene dosage and there is a striking phenotypic similarity between *Pax6* and *Foxe3* mutants. We therefore propose that many of the ocular malformations associated with *Pax6* haploinsufficiency are consequences of a reduced expression of *Foxe3*.

Keywords: Forkhead; Lens; Cataract; Aphakia

Introduction

For over a century, lens formation has been the classical example of induction and in the last two decades the molecular mechanisms behind differentiation and morphogenesis of the lens have begun to be understood. A master gene of eye development is *Pax6*, and although it is expressed in both the inducing optic vesicle and the responding ectodermal cells, genetic and tissue recombination experiments have demonstrated that it is its ability to confer lens forming competence to the presumptive placode cells that is crucial for its role in lens development (Collinson et al., 2000; Davis-Silberman et al., 2005; Dimanlig et al., 2001; Fujiwara et al., 1994; Quinn et al., 1996). The combined action of Pax6 in pre-placode cells and inducing factors—including Bmp and Fgf (reviewed by Lang, 2004)—from the optic vesicle, triggers activation of a set of transcription factors which mediate the differentiation and morphogenesis that lead to lens formation. These include Prox1, essential for lens fiber differentiation and cell cycle exit (Wigle et al., 1999); Mab21l1, drives proliferation and invagination in the lens placode (Yamada et al., 2003); Sox proteins, activators of crystallin gene expression (Kamachi et al., 2001); Six3, maintains—by mutual activation—expression of *Pax6* (Goudreau et al., 2002); and Foxe3, the subject of this article.

Transcription of *Foxe3* is activated in the early lens placode around E9, stays on in the entire lens vesicle up until about E12.5, when it is switched off in the differentiating primary lens fibers (Blixt et al., 2000). Expression persists in the anterior lens epithelium throughout life and this tissue requires Foxe3 for maintenance, proliferation and survival (Blixt et al., 2000). The *dysgenetic lens* (*dyl*) mouse mutant (Sanyal and Hawkins, 1979) has two amino acid substitutions in the forkhead (DNA binding) domain of Foxe3, which co-segregate with the *dyl* phenotype (Blixt et al., 2000) and destroys the protein's binding to its cognate site in DNA (Ormestad et al., 2002).

In addition to maintaining the lens epithelium in an actively proliferating, undifferentiated state, *Foxe3* is also required for closure of the lens vesicle; in *dyl* mice, the lens pit stays as an urn-

* Corresponding author. Fax: +46 31 7733801.
E-mail address: peter.carlsson@molbio.gu.se (P. Carlsson).

0012-1606/$ - see front matter © 2006 Elsevier Inc. All rights reserved.
doi:10.1016/j.ydbio.2006.09.021

shaped structure, continuous with the surface ectoderm that will later form the corneal epithelium (Blixt et al., 2000; Sanyal and Hawkins, 1979). A milder version of this defect occurs, with incomplete penetrance, in *Foxe3* heterozygotes in the form of a persistent connection between lens and cornea, or remnants of lens material inside the central corneal stroma (Ormestad et al., 2002). This malformation overlaps with the clinical manifestations of Peters' anomaly, and two human cases of anterior segment dysgenesis have been reported to be heterozygous for mutations in *FOXE3* (Ormestad et al., 2002; Semina et al., 2001).

Here, we confirm that the mutations in *Foxe3* are responsible for the *dyl* phenotype by showing that a targeted deletion of the *Foxe3* forkhead box phenocopies *dyl*. We also investigate the consequences of inactivation of *Foxe3* for development of the anterior segment of the eye, and the response of *Foxe3* expression to altered *Pax6* gene dosage, in the light of similarities between *Pax6* and *Foxe3* haploinsufficiency phenotypes.

Materials and methods

Targeting Foxe3

A targeting construct containing a total of 8.9 kb of the *Foxe3* locus was made from overlapping 129/Sv genomic λ clones. The forkhead box of *Foxe3* (from *Nco*I to *Not*I) was replaced by a *lacZ-PGK-Neo*^{R} cassette and the HSV-*tk* gene was appended to the short arm of the construct for negative selection. The construct was linearized at the end of the long arm and electroporated into R1 ES cells. Colonies resistant to 300 μg/ml G-418 and 2 μM ganciclovir were screened by Southern blot with two probes. The first probe is located outside the short (2.2 kb) arm of the targeting construct (5′ of *Foxe3*) and identifies fragments beginning at an external *Sac*I site and ending at *Sac*I sites downstream of the forkhead box (*wt* allele, 8.7 kb) or within the *lacZ-PGK-Neo*^{R} cassette (targeted allele, 6.5 kb). The other probe is located within the long (6.7 kb) arm and identifies the same *Sac*I fragment as the short arm probe (wt allele, 8.7 kb), and a fragment from a *Sac*I site within the *lacZ-PGK-Neo*^{R} cassette to a site within the long arm (targeted allele, 7.4 kb). Homologous recombination between the targeting construct and the *Foxe3* locus occurred with a frequency of 7% of Neo^R colonies. Targeted cell clones were used to generate chimeras through injection into C57Bl/6 blastocysts. A knockout line was established following germline transmission of targeted ES cells and made congenic with the *dyl* (Sanyal and Hawkins, 1979) strain by crossing with Balb/c for five generations. Genotyping of tail biopsies or embryos was performed by Southern blot, or by PCR using a common primer located upstream of the forkhead box, combined with either a primer specific for the *wt* allele, or a primer in *lacZ*, specific for the targeted allele.

Mouse strains

The *dyl* mutant, which arose spontaneously in the Balb/c strain (Sanyal and Hawkins, 1979), was obtained from The Jackson Laboratory (Bar Harbor, Maine). The *Small eye* (*Sey*) mutant was kindly provided by Dr H. Edlund (Umeå, Sweden), but comes originally from Dr V. van Heyningen (Edinburgh, UK). We obtained it on an impure C57Bl/6 background and have transferred the allele to Balb/c; the animals used here have at least five generations on this genetic background. PCR genotyping of the *Pax6*^{Sey} and *Foxe3*^{dyl} alleles was performed as previously described (Blixt et al., 2000; Grindley et al., 1995). Balb/c mice as wild-type controls and for breeding of mutants were purchased from Charles River Inc. (Germany).

Histology, in situ hybridization and immunohistochemistry

In situ hybridization of whole-mount mouse embryos and cryosections (8 μm) with *Foxe3* and *Cryaa* probes were performed as previously described (Blixt et al., 2000). A minimum of four embryos of each genotype and developmental stage were analyzed by whole-mount *in situ* hybridization. For immunohistochemistry and hematoxylin–eosin staining, eyes were fixed in 4% paraformaldehyde and processed for paraffin embedding and sectioning (5 μm). Glutaraldehyde fixation, followed by epoxy resin embedding, was used for thin (1 μm) histological sections (stained with Richardson's methylene blue/azur II) and electron microscopy (TEM). The rabbit polyclonal anti-Foxe3 antiserum was directed against a peptide corresponding to the carboxyterminal 19 amino acids of murine Foxe3. N-cadherin was stained with a mouse monoclonal antibody (Clone 3B9; Zymed, 33-3900) using "The Ark" mouse-on-mouse kit from Dako and antigen retrieval by treatment with Tris–EDTA buffer in a pressure boiler. ZO-1 was detected with a rabbit polyclonal antiserum (Zymed, 61-7300) after antigen demasking with Type XIV protease (Sigma), 2 mg/ml, 10 min, 37°C. Binding of antibodies was visualized with streptavidin–HRP, DAB and signal amplification with a TSA kit (Perkin Elmer).

Volume measurements

Embryos with 33±1 somites were selected from E10.5 litters of different genotypes, paraffin embedded and sectioned. Lens tissue volume was calculated by integration of area measurements from serial sections, using an Zeiss Axioplan 2 microscope and the area measurement function of the AxioVision software.

Results

Targeted deletion of Foxe3 phenocopies dysgenetic lens (dyl)

To settle if the mutation in *Foxe3* that we previously found in the *dysgenetic lens* (*dyl*) strain (Blixt et al., 2000; Sanyal and Hawkins, 1979) is responsible for the mutant phenotype and, if so, whether it represents a null mutation, we created a targeted deletion of the forkhead box in *Foxe3* (Fig. 1). To minimize the effects of differences in genetic background, the *Foxe3*^{tm} line was made congenic with the *dyl* strain by crossing with Balb/c for five generations. Mice homozygous for the targeted allele (*Foxe3*$^{tm/tm}$) showed the characteristic fusion between cornea and a small, severely cataractic lens, as previously described for the *dyl* mutant. Offspring from crosses between *dyl* and knockout mice (*Foxe3*$^{tm/dyl}$) were phenotypically indistinguishable from the (homozygous) parental strains at all embryonic and postnatal stages examined (Fig. 2), which formally proves that *dyl* is an allele of *Foxe3*. It also supports our prediction, based on inability of the Foxe3^{dyl} protein to bind DNA, that *Foxe3*^{dyl} is a null allele (Blixt et al., 2000; Ormestad et al., 2002).

Immunohistochemistry with an antiserum directed against the carboxyterminal end of Foxe3 showed intense nuclear staining in the lens epithelium of wild-type and *dyl* E14.5 embryos, but no detectable staining in the knockout (Figs. 2C, F, I). Beside confirmation of successful inactivation of Foxe3 in the targeted allele, this indicates that the Foxe3^{dyl} protein is stable and nuclear, which supports the notion that it is the failure to bind DNA that is responsible for the loss-of-function phenotype.

Foxe3 is important for differentiation of anterior segment mesenchyme

Transplantation experiments in chick embryos showed the anterior surface of the lens, i.e., the lens epithelium, to be important for corneal development (Beebe and Coats, 2000; Genis-Galvez, 1966; Genis-Galvez et al., 1967; Zinn, 1970).

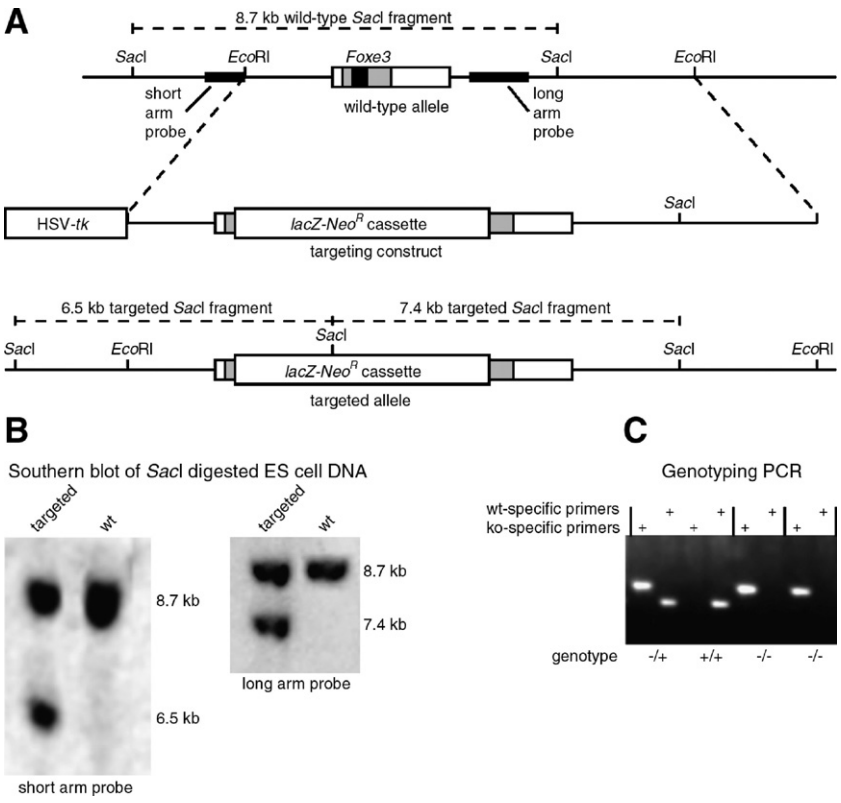

Fig. 1. Targeting the *Foxe3* locus. (A) Schematic showing knockout strategy, location of probes for Southern blot and predicted sizes of restriction fragments used for mapping. The intron-less *Foxe3* gene is depicted with the open box representing the transcribed region, the shaded the coding sequence, and the black the forkhead box, which is deleted in the targeting construct. (B) Screening of ES cell clones by Southern blot hybridization. (C) Genotyping by PCR of offspring from crosses between two $Foxe3^{tm/+}$ mice.

We therefore made a detailed analysis of the anterior segment–cornea, iris, ciliary body and filtration angle–in *Foxe3* mutant mice. Both $Foxe3^{tm/tm}$ and $Foxe3^{dyl/dyl}$ strains were analyzed in order to detect signs of residual activity of the $Foxe3^{dyl}$ protein, but no consistent differences between the two could be detected. Hence, they will be collectively referred to as $Foxe3^{-/-}$.

As described previously, the most striking malformation in the homozygous *Foxe3* mutant, beside the rudimentary lens, is the persistent connection between lens and cornea, caused by failure of the lens vesicle to close and separate from the surface ectoderm (Blixt et al., 2000; Sanyal and Hawkins, 1979). In adults, this connection is sometimes broken (Figs. 2E, H), but leaves behind a deposit of tissue derived from the interior of the lens vesicle on the central part of the external corneal surface, as well as inside its stroma (Fig. 2), which affects the histology of the central part of the cornea. The corneal stroma was lax with a reduction in the number and density of collagen fibers (Fig. 3). The stratification of the cornea is less pronounced, as seen for example in the distribution of ZO-1, a component of tight junctions normally present at high density in the epithelium and endothelium of the cornea, but not in the stroma (Fig. 4). In $Foxe3^{-/-}$ ZO-1 staining was more or less equally distributed across the cornea.

Iris and ciliary body are both made up of a double epithelium–an extension of the optic cup/retina–and a mesodermal stroma (Gage et al., 2005). In *Foxe3* null mice, iris and ciliary body are replaced by a single, simple structure that resembles a stunted iris (e.g., Figs. 2E, H, K; 4B; 5C). Its relationship with ciliary processes is shown by the presence of zonular fibers reaching between its posterior surface and the lens (Fig. 5F), but like an iris its anterior surface is made up of stromal cells. Histologically it resembles neither iris, nor ciliary body (Figs. 5F, I). Both the stromal and epithelial parts are compact and fairly homogenous; they lack the muscle cells, blood vessels, nerves and the intricate channels of extracellular space characteristic of a normal iris, as well as the secretory apparatus, fenestrated capillaries and musculature of the ciliary body.

The trabecular meshwork of the filtration angle and the corneal endothelium are other derivatives of the periocular mesenchyme. In *Foxe3* mutants neither filtration angle, nor corneal endothelium develop normally. Instead, the compact stroma of the fused iris/ciliary body continues along the inner surface of the cornea (Figs. 3D; 5L). As a result, the filtration angle is severely malformed and without trabecular meshwork (Fig. 5L). The status of the Canal of Schlemm in *Foxe3* mutants is difficult to evaluate; the iridocorneal angle is severely malformed and ruptures in the tissue frequently occur, but in most sections it appears to be missing. The presence of Descemet's membrane in *Foxe3* null mice (Fig. 3H) suggests that the tissue layer covering the inner surface of the corneal stroma have functional characteristics of endothelial cells, in spite of their abnormal histology. In place of the normal endothelial monolayer, the inner corneal surface is covered by a crowded and disorganized layer of cells that histologically resembles the stroma cells of the fused iris/

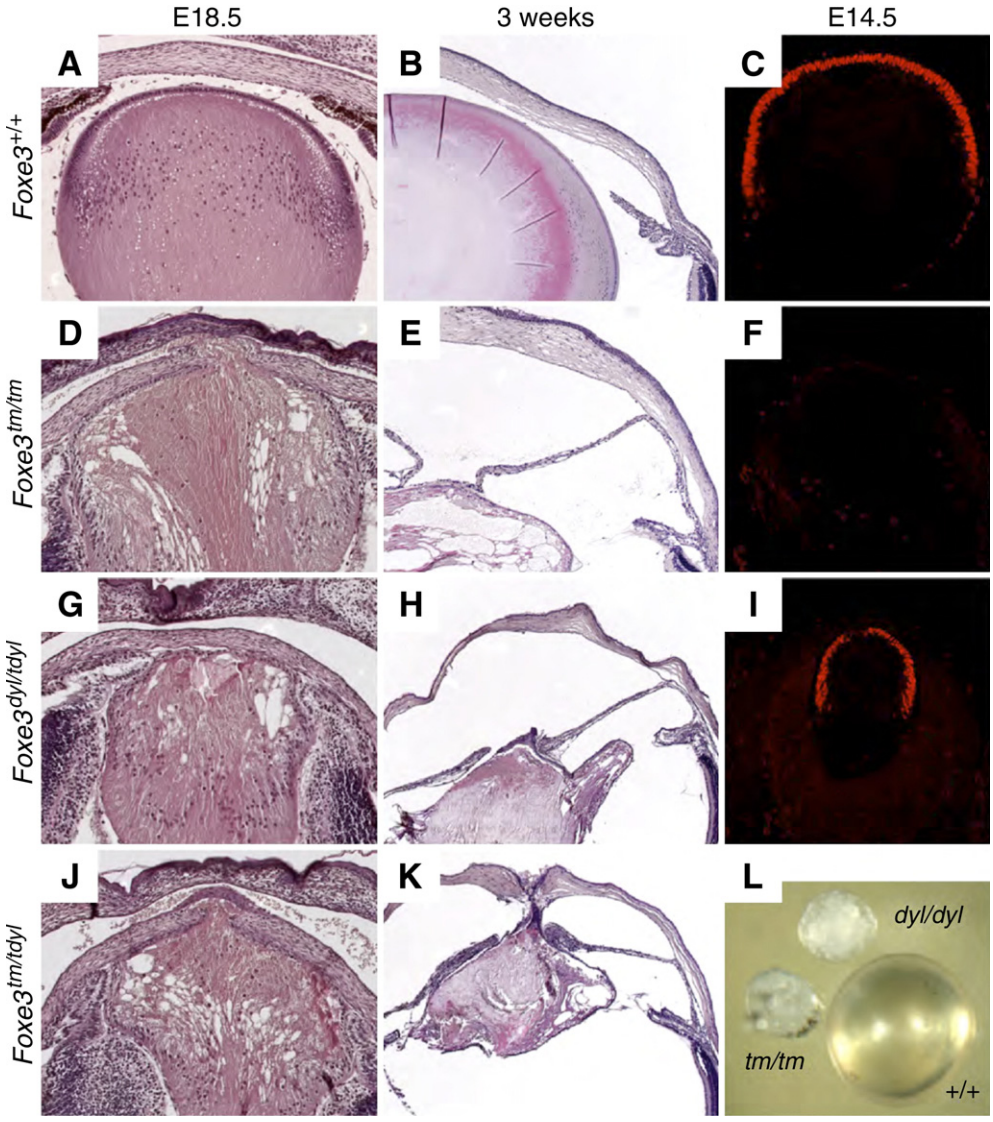

Fig. 2. Targeted deletion of *Foxe3* phenocopies the *dysgenetic lens* (*dyl*) mutant. Phenotype of, and Foxe3 protein distribution in, wild type (A–C); *Foxe3*$^{tm/tm}$ (D–F); *Foxe3*$^{dyl/dyl}$ (G–I); and *Foxe3*$^{tm/dyl}$ (J, K). H&E stained sections of eyes from E18.5 embryos (A, D, G, J) and 3-week-old mice (B, E, H, K). Immunofluorescence with antiserum against the C-terminus of Foxe3 on sections from E14.5 embryos (C, F, I). Panel (L) shows intact lenses from 3-week-old wild-type, *Foxe3*$^{tm/tm}$ and *Foxe3*$^{dyl/dyl}$ mice.

ciliary body (Figs. 3D, H). A high content of melanosomes—normally present in iris stroma, but not in corneal endothelium—is characteristic of these cells (Fig. 3H), and they frequently adhere to the "iris/ciliary body stroma" (Figs. 5F, L). Adherence between cell populations that normally do not interact physically, suggested altered expression of cell adhesion proteins. We therefore examined the distribution of N-cadherin, a cell adhesion molecule normally present in corneal endothelium and lens, but not in iris stroma. It is highly expressed in retina and ciliary body epithelium, but only in minute amounts in iris epithelium (Figs. 4A, C, E, G, Beebe and Coats, 2000; Reneker et al., 2000). In *Foxe3* null mice N-cadherin is present in all mesenchyme facing the anterior chamber—including that of the rudimentary iris/ciliary body—which explains the extensive adherences between these cell populations (Figs. 4B, D, F).

Foxe3 is essential for survival, proliferation and maintenance of the lens epithelium (Blixt et al., 2000). Therefore, it is impossible to tell if the malformations and misdifferentiation of the anterior segment in *Foxe3* null mutants are consequences only of the absence of a lens epithelium, or if Foxe3 plays a more direct role. However, in mature *Foxe3*$^{-/+}$ mice the lens epithelium appears grossly normal and any defects in the differentiation of iris, cornea, filtration angle or ciliary body in these animals would suggest that Foxe3 is directly involved in control of secreted factors required for normal development of the anterior segment.

We previously described that keratolenticular adhesion and/or leukoma occur in *Foxe3*$^{dyl/+}$ mutants with a penetrance of approximately 40% in the Balb/c strain (Ormestad et al., 2002). These adherences appear to be a less severe version of the failed lens vesicle closure seen in

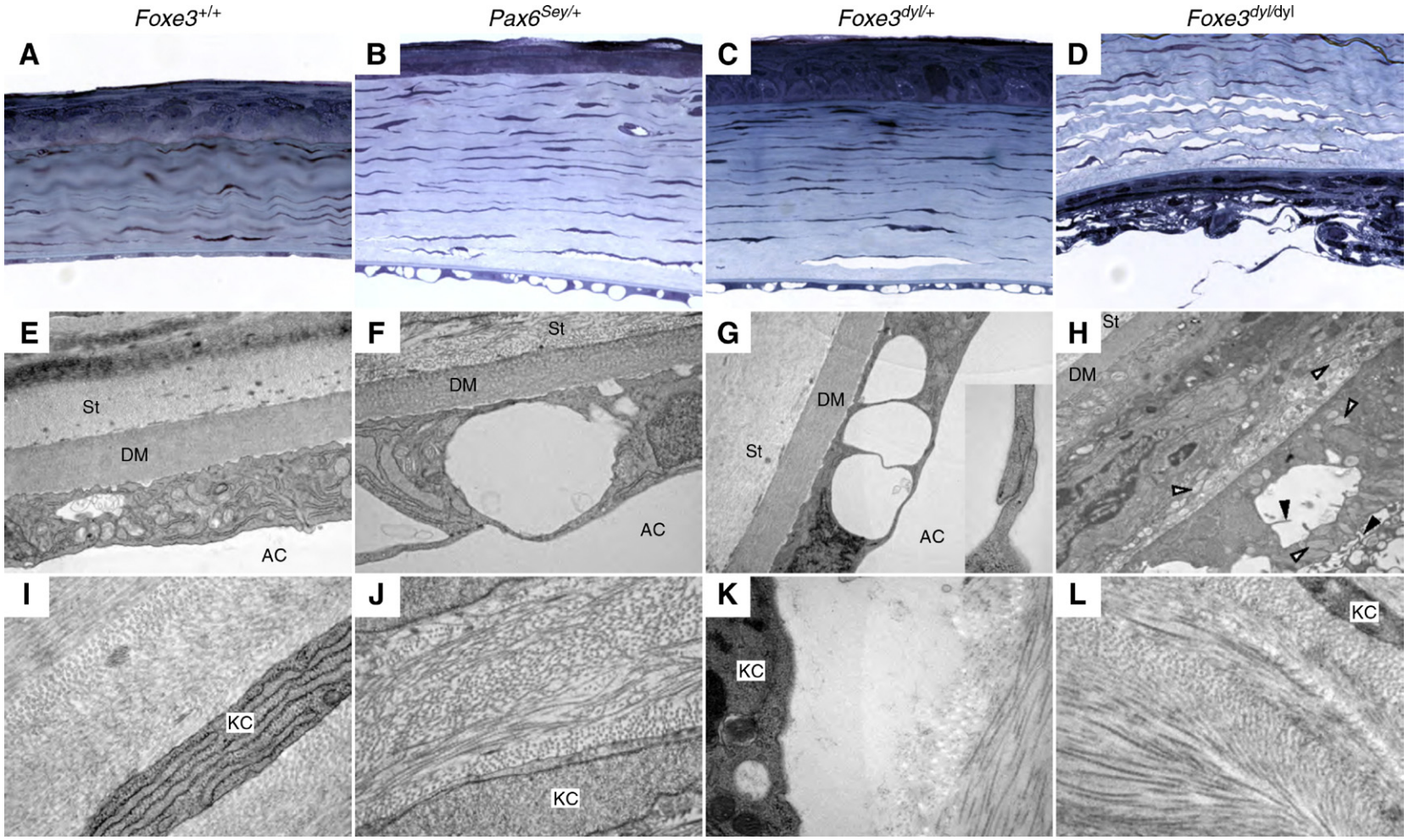

Fig. 3. Similar cornea defects in *Foxe3*$^{dyl/+}$ and *Pax6*$^{Sey/+}$ mice. Light microscopy (A–D) and TEM (E–L) images of cornea from 3-week-old wild-type (A, E, I); *Pax6*$^{Sey/+}$ (B, F, J); *Foxe3*$^{dyl/+}$ (C, G, K); and *Foxe3*$^{dyl/dyl}$ (D, H, L) mice. The wild-type corneal stroma ("St") consists of highly ordered collagen bundles in alternating angles, with fixed dimensions and distances; and thin keratocytes ("KC"), densely packed with rough ER membranes (I). The stroma of *Pax6*$^{Sey/+}$ (J), *Foxe3*$^{dyl/+}$ (K), and *Foxe3*$^{dyl/dyl}$ (L) mutants show signs of edema: loose, divergent collagen fibers and liquid filled gaps between collagen bundles (or between keratocytes and the collagen as seen in panel K). Descemet's membrane ("DM") is present in all genotypes (E–H)—although slightly thinner in mutants—which implies that the corneal endothelium is functional, at least in terms of production of basal lamina components, in *Foxe3*$^{-/-}$ (H) mutants. Adjacent endothelial cells are separated by inflated gaps in *Foxe3*$^{-/+}$ (C, G) and *Pax6*$^{Sey/+}$ (B, F) corneas. These "bubbles" are delimited from the anterior chamber by thin membrane folds kept together by tight junctions (high magnification inset in panel G). The corneal endothelium of *Foxe3*$^{-/-}$ mutants is lax and multilayered (D), and contains many melanosomes (white arrowheads in panel H; albino mice—therefore not pigmented). It is also interrupted by channels of extracellular space into which microvilli (black arrowheads in panel H) protrude—structures characteristic of the normal iris stroma—and is strikingly different from the polarized endothelial monolayer of the wild type (A, E).

Foxe3 null mice and do not necessarily tell us anything about the role of Foxe3 in the inductive properties of the lens epithelium. A closer inspection did, however, reveal a range of additional defects in the anterior segment of heterozygous mice, several of which imply differentiation errors in cell types that develop long after the lens vesicle has closed. Most conspicuous are the many adherences between, for example, lens and iris (Fig. 5E). Extensive adherence between iris stroma and cornea endothelium results in closure of the filtration angle along parts of the ocular circumference (Fig. 5K).

The iris of *Foxe3* heterozygotes is generally thinner and less well developed than in wild type (Figs. 5D, E). An important function of the iris is to exchange gases, nutrients and waste products with the aqueous humor in order to support the non-vascularized tissues of the anterior segment. This is facilitated by a generous blood supply and a surface-increasing microanatomy of both stroma and epithelium, particularly obvious through the electron microscope. The heterozygous iris is more compact and lacks the intricate channels of extracellular space that penetrate deep into the wild-type iris (Figs. 5G, H). Blood vessels in the corneal stroma are a sign of hypoxia and suggest that the simpler structure of the iris may compromise its ability to oxygenate the aqueous humor. The corneal endothelium of the mutant is filled with large "bubbles" (Fig. 3C). TEM revealed that these consist of inflated extracellular space in between endothelial cells, and are delimited from the anterior chamber by tight junctions (Fig. 3G). The corneal stroma show clear signs of edema with disorganized, loosely packed collagen fibers (Figs. 3C, K).

Iris hypoplasia, keratolenticular adhesion and various other anterior segment malformations have been reported also in *Pax6* mutants (*Sey*) (Baulmann et al., 2002; Davis et al., 2003; Hill et al., 1991; Hogan et al., 1986; Ramaesh et al., 2003; Theiler et al., 1978). We therefore compared congenic (>5 generations on Balb/c) $Pax6^{Sey/+}$ mice with $Foxe3^{-/+}$. The similarity was striking: blood vessels in the cornea; a "bubbly" corneal endothelium; corneal edema with deranged collagen bundles; a thinner iris; and angle closed by iridocorneal adhesion (Fig. 3B, F, J, Baulmann et al., 2002; Davis et al., 2003; Ramaesh et al., 2003). Iris hypoplasia is more severe in $Pax6^{Sey/+}$ than in $Foxe3^{-/+}$, but the overall range and character of malformations are so similar that they suggest a common mechanism.

Lens expression of Foxe3 is sensitive to Pax6 gene dosage

Although *Pax6* is involved in many differentiation processes and homozygous null embryos have malformations in the CNS and in nasal structures, the anterior segment of the eye is particularly sensitive to *Pax6* gene dosage. *Pax6* expression is normal in $Foxe3^{-/-}$ during the early stages of lens development (ÅB and PC, unpublished), but the many phenotypical similarities between *Foxe3* and *Pax6* mutants suggested that a reduction in *Foxe3* expression might be responsible for the anterior segment defects in $Pax6^{Sey/+}$.

Brownell et al. (2000) showed that in $Pax6^{Sey/Sey}$ embryos no activation of *Foxe3* takes place in the surface ectoderm. However, since no lens induction or placode formation occur in this mutant, this could reflect the absence of placode cell differentiation as well as a more direct requirement for *Pax6*. To investigate if *Foxe3* is sensitive to Pax6 gene dosage, we analyzed *Foxe3* expression in wild-type, $Pax6^{Sey/+}$ and $Pax6^{Sey/Sey}$ E10.5 embryos by whole-mount *in situ* hybridization. In wild type, *Foxe3* mRNA is first detected in lens placode and posterior diencephalon around E9 (Blixt et al., 2000). At E10.5, high expression is seen in the lens vesicle together with weaker, localized expression in the brain (Fig. 6A). *Foxe3* mRNA could not be detected in the surface ectoderm overlying the optic vesicles of $Pax6^{Sey/Sey}$ embryos at E10.5 (Fig. 6C), in agreement with the results of Brownell et al. (2000). Neither did we detect any expression in the brain of homozygous *Pax6* mutants, which suggests that Pax6 is required for *Foxe3* expression in both tissues.

In $Pax6^{Sey/+}$ heterozygous embryos, the distribution and level of *Foxe3* expression in the brain was indistinguishable from that of wild-type siblings (Fig. 6B). However, the heterozygous embryos showed a dramatic reduction of *Foxe3* mRNA in lens placode, pit and vesicle. At E10.5, the hybridization signal is barely detectable in the mutant (Figs. 6B, E), but very strong in the wild-type (Figs. 6A, D). At E11.5 the difference is less dramatic, but still obvious (Figs. 6F, G). In embryos with the same number of somites, the lens pit or vesicle is smaller in $Pax6^{Sey/+}$ than in wild type (Figs. 6E, L, van Raamsdonk and Tilghman, 2000), but it is clear that the difference in *Foxe3* expression is not just a consequence of a delay in lens development, nor of a reduction in the number of expressing cells; wild-type embryos have high levels of *Foxe3* mRNA in the lens placode before invagination of the lens pit begins, whereas in $Pax6^{Sey/+}$ heterozygotes no or little expression can be detected as late as E10.5, when the lens pit is already well defined.

To investigate if the drop in *Foxe3* expression reflected a general delay in activation of lens markers, we examined the expression of *Cryaa*, encoding α-A-crystallin. *Cryaa* expression is gradually activated during formation of the lens anlage and becomes easily detected between E10.5 and 11.5, at about the time when the lens vesicle closes. In E10.5 embryos, *Cryaa* mRNA was very low in wild-type and $Pax6^{Sey/+}$, but at E11.5 high expression was seen in the lens vesicles of both genotypes (Figs. 6H–K). Thus, *Cryaa* activation is synchronous in heterozygous and wild-type embryos and apart from the mutant vesicle being smaller, neither morphological, nor gene expression data provide any evidence for a general delay in lens induction or development. A plausible explanation for the low *Foxe3* expression in the lens anlage of $Pax6^{Sey/+}$ heterozygous embryos is therefore a non-linear response of the *Foxe3* promoter to variations in Pax6 concentration.

A prediction from the hypothesis that reduced *Foxe3* expression is responsible for the sensitivity of the anterior segment to a decreased *Pax6* gene dosage, is that the smaller lens vesicle size observed in $Pax6^{Sey/+}$ should be phenocopied in *Foxe3* mutants. To address this, we measured the volume of the lens vesicle tissues of somite-matched E10.5 embryos by

integrating from area measurements of serial sections. The conclusions that can be drawn are limited by the small sample size, but as shown in Fig. 6L, the reduction in lens vesicle tissue volume is within the same range for *Foxe3*$^{dyl/dyl}$ and *Pax6*$^{Sey/+}$, whereas *Foxe3*$^{dyl/+}$ embryos were intermediate between these and wild type.

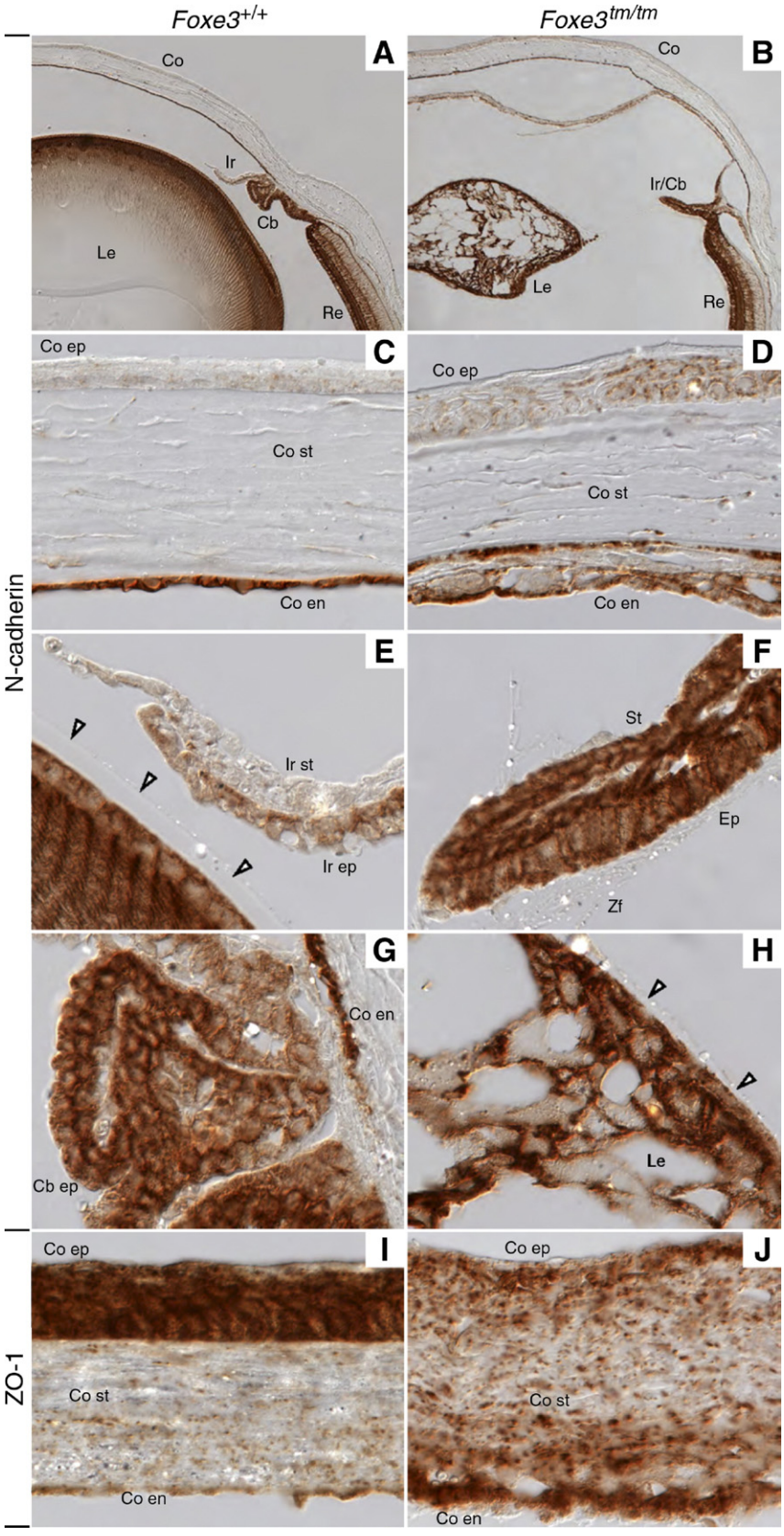

Discussion

Foxe3^{dyl} is a null allele

At all embryonic and postnatal stages examined, we were unable to detect any consistent difference between *Foxe3$^{dyl/dyl}$*, *Foxe3$^{tm/tm}$* and *Foxe3$^{tm/dyl}$*. This supports our initial prediction (Blixt et al., 2000) that the amino acid substitutions in Foxe3^{dyl} inactivates the protein. It is also in agreement with the observed inability of Foxe3^{dyl} to bind DNA (Ormestad et al., 2002). Medina-Martinez et al. (2005) concluded that *Foxe3^{dyl}* is a hypomorphic allele, based on claims of differences between the phenotypes of *Foxe3$^{dyl/dyl}$* and mice homozygous for a targeted allele. As no direct comparison with the *dyl* mutant was presented, it is unclear on what this conclusion was based. Furthermore, since the animals carrying the targeted allele had a mixed 129×C57Bl/6 background and the *dyl* strain is inbred Balb/c, it is difficult to asses to what extent for example the reported absence of corneal endothelium reflects strain differences, or misinterpretation of this overgrown tissue as a multilayered lens epithelium. However, we found that when congenic *Foxe3$^{dyl/dyl}$* and *Foxe3$^{tm/tm}$* strains were compared, any phenotypic difference between them is at least dwarfed by the stochastic, interindividual variation.

Foxe3 directly influences anterior segment morphogenesis and differentiation

In the absence of functional Foxe3, tissues derived from the periocular mesenchyme retain a simple histology, instead of differentiating into proper corneal endothelium, trabecular meshwork and the many specialized cell types of iris and ciliary body stroma. This "default" mesenchyme expresses N-cadherin throughout—a cell adhesion molecule normally present in the corneal endothelium and lens, but not in iris. The expanded N-cadherin expression in murine *Foxe3* null mutants may explain the frequent adherences between different parts of the anterior segment, but contrasts with the absence of corneal endothelium and N-cadherin in chick embryos from which the lens has been removed, or turned (Beebe and Coats, 2000). There are several possible reasons for this discrepancy. First, the paracrine signaling pattern of a *Foxe3$^{-/-}$* lens is likely to be different from a normal lens turned around, or from no lens at all. Secondly, interspecies differences between mouse and chicken include both the origin (Gage et al., 2005) and the differentiation mechanism (Kidson et al., 1999) of the corneal endothelium.

The goniodysgenesis caused by loss of one *Foxe3* allele, with the filtration angle partially closed by iridocorneal adherence, suggests that *FOXE3* could be a genetic factor in human developmental glaucoma. Other murine phenotypes described here that may be relevant from a clinical ophthalmological point of view, and for which *FOXE3* should be considered a candidate gene, include iris hypoplasia, corneal edema, leukoma, and various adherences involving lens, iris and cornea.

The main function of the corneal endothelium is to form a tight barrier between the stroma and the anterior chamber. Endothelial cells pump ions from the former to the latter, thereby creating the osmotic gradient that keeps the stroma dehydrated and optically clear (Arffa, 1998). Any disturbance of the integrity of the endothelium therefore leads to edema, corneal swelling and opacity. That the structural abnormalities in the corneal endothelium observed in *Foxe3* heterozygotes influences its function is confirmed by the overt edema of the stroma with leukoma, disorganized collagen fibers and liquid-filled gaps. The bubbles in the endothelium that are common in both *Foxe3$^{-/+}$* and *Pax6$^{Sey/+}$* consist of space between the lateral membranes of adjacent cells, apparently filled with liquid under higher pressure than the aqueous humor. They are enabled by intact tight junctions close to the apical surface and suggest that ion pumps that should be restricted to the apical membrane are mislocated to the lateral. The simplest, although purely hypothetical, explanation for this abnormality is therefore that Foxe3 controls the production of factors secreted to the aqueous humor by the lens epithelium that are important for polarization of corneal endothelial cells. Incomplete polarization leads to mislocation of membrane proteins, with ions being pumped laterally—and perhaps also basically—instead of just apically. The net flux of ions and water from the stroma to the anterior chamber would be compromised and corneal edema would follow.

The ring-like structure around the lens in *Foxe3$^{-/-}$* mice may be regarded as a simple ciliary process with epithelium only on its posterior surface, or as a stunted iris with ectopic zonular fibers. Likewise, the unstructured tissue covering the interior surface of the cornea, but often partially detached and adhering to the lens, may be regarded as an overgrown corneal endothelium, or as an iris stroma devoid of epithelium. Either way, the conclusion is that in the absence of functional Foxe3 all tissues derived from the periocular mesenchyme and directly facing the anterior chamber are severely dysplastic and—in terms of cell adhesion properties, N-cadherin expression and ultrastructure—quite uniform.

After submission of this paper, Valleix et al. (2006) reported about three siblings from a consanguineous family with congenital primary aphakia linked to homozygosity for a premature stop codon in *FOXE3*. The truncation leaves the

Fig. 4. Widespread ectopic expression of N-cadherin in the anterior segment of *Foxe3$^{-/-}$* eyes. Immunohistochemistry with antibody against N-cadherin (A–H) and zonula occludens 1 (ZO-1; I, J) on sections from eyes of three weeks old wild-type (A, C, E, G, I) and *Foxe3$^{-/-}$* (B, D, F, H, J) mice. In wild type, N-cadherin is abundant in retina ("Re"; A), ciliary body epithelium ("Cb ep"; G), corneal endothelium ("Co en"; C, G), and lens (both epithelium and fibers; "Le"; A, E). It is absent in the stroma of both iris and ciliary body ("Ir st"; E), and present in minute amounts in iris epithelium ("Ir ep"; E). In the *Foxe3* null mutant, N-cadherin is abundant in all tissues facing the anterior chamber, including both epithelium ("Ep"; F) and stroma ("St"; F) of the "iris/ciliary body" ("Ir/Cb"; B, F) and in the overgrown corneal endothelium ("Co en"; D). The thickness of the lens capsule (arrowheads in panel E) is reduced and more variable in the mutant (arrowheads in panel H). Differentiation of all corneal layers are affected in the *Foxe3* mutant, as seen in the poor stratification in the occurrence of the tight junction protein ZO-1 (J), normally confined to epithelial and endothelial cells (I). Abbreviations: Cb, ciliary body; Co, cornea; panel Co ep, corneal epithelium; Co st, corneal stroma; Ir, iris; Zf, zonular fibers.

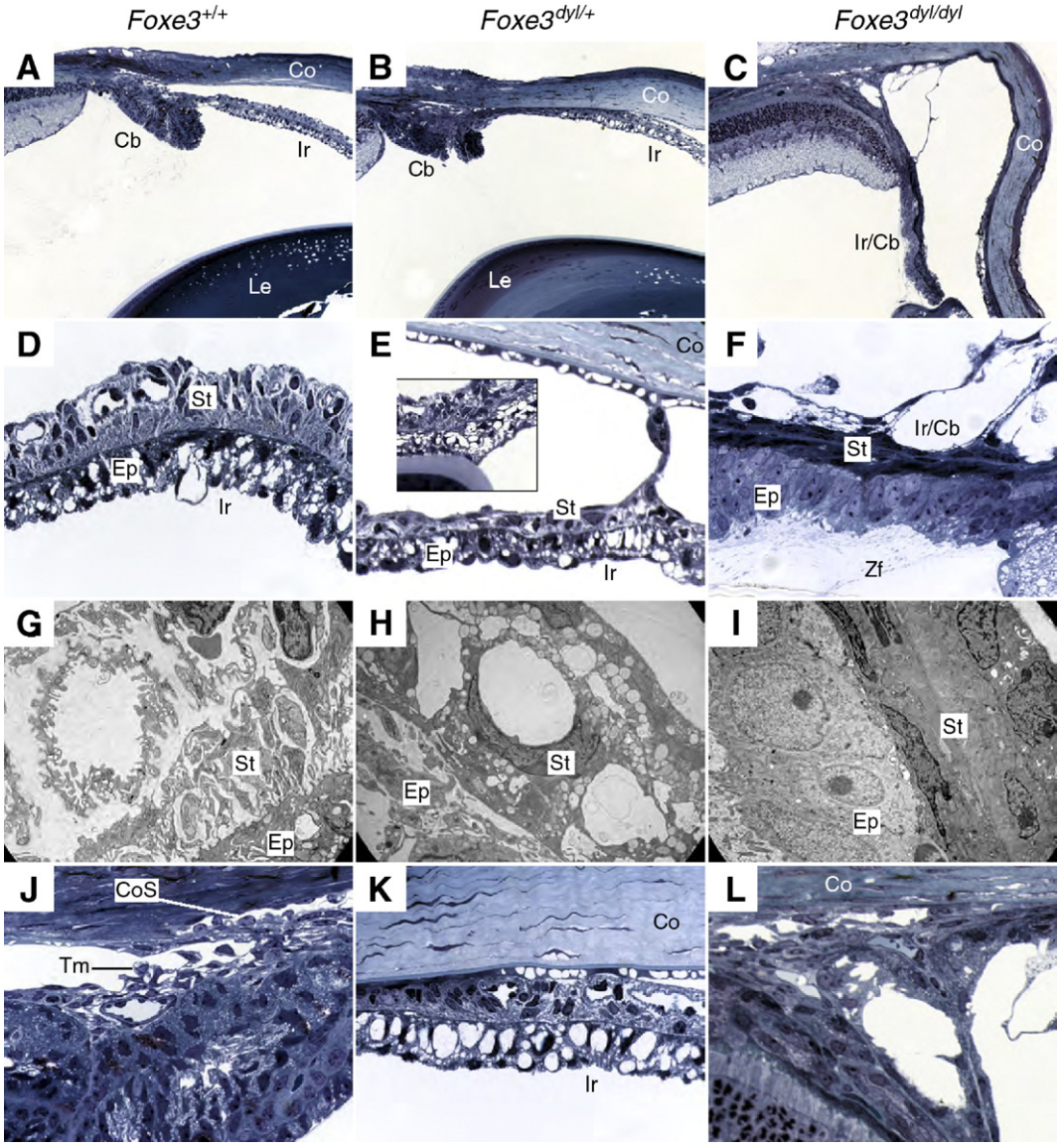

Fig. 5. Defective differentiation of iris and iridocorneal angle in *Foxe3* mutants. Light microscopy (A–F; J–L) and TEM (G–I) images. In wild-type mice at three weeks of age (A, D, G, J), the angle between iris and cornea contains a trabecular meshwork ("Tm"; A, J), which filters the aqueous humor that drains through the Canal of Schlemm ("CoS"; J). Both epithelial ("Ep") and stromal ("St") layers of the iris have an intricate morphology with a complex, surface-increasing microanatomy; channels of extracellular space penetrate deep into the tissue in a system of branched channels and folds ("Ir"; D, G). In *Foxe3* null mutants (C, F, I, L) neither filtration angle, nor iris, develop normally. In place of ciliary body and iris, a single, simple structure is formed which consists of a posterior epithelial and an anterior stromal layer (C, F, I). The relationship with ciliary processes is shown by the presence of zonular fibers, which connect the epithelial cells with the lens ("Zf"; F), but like an iris the anterior surface is made up of stromal cells. However, the histology of both layers is dense and lacks the intricacy of the normal iris (F, I). The compact stroma continues onto the inner surface of the cornea without any obvious change in histology; thus none of the structures of a normal filtration angle are formed (C, L). Strong cohesion between the cells on either side of the "angle" illustrates that the differentiation of cell adhesion properties that normally prevents adherence between iris and the surrounding tissues has failed (C, F, L). Abnormal adherences are frequent, although much less severe, also in *Foxe3* heterozygotes and include irido-corneal (B, E, K) and irido-lenticular (inset in panel E) connections. Fusion between peripheral iris and corneal endothelium leads to closure of the filtration angle (B, K). The iris of heterozygotes is thinner, denser (E) and has a simpler microanatomy (H).

DNA binding domain of FOXE3 intact, but removes 80 amino acids from the C-terminus. Since *FOXE3* is a single exon gene, nonsense mediated decay (NMD) is not expected and the predicted truncated protein may well be produced in normal levels. The eye defects are very similar to those of the mouse null mutants described here, but appear even more severe, with reported absence of lens, iris, ciliary body, trabecular meshwork, Descemet's membrane and Schlemm's canal. The affected child for which post mortem tissue was available for analysis, had—like the mouse mutant—the inner surface of the cornea covered by multiple cell layers containing melanosomes. The differences between the human cases and the mouse null mutants may reflect species differences, or a dominant effect of the truncated protein in the human case.

In addition to the lens, *Foxe3* is also expressed in a small area of the dorsolateral diencephalon during a brief period of embryonic development. The functional significance of this, if any, remains unknown and null mice do not exhibit any obvious

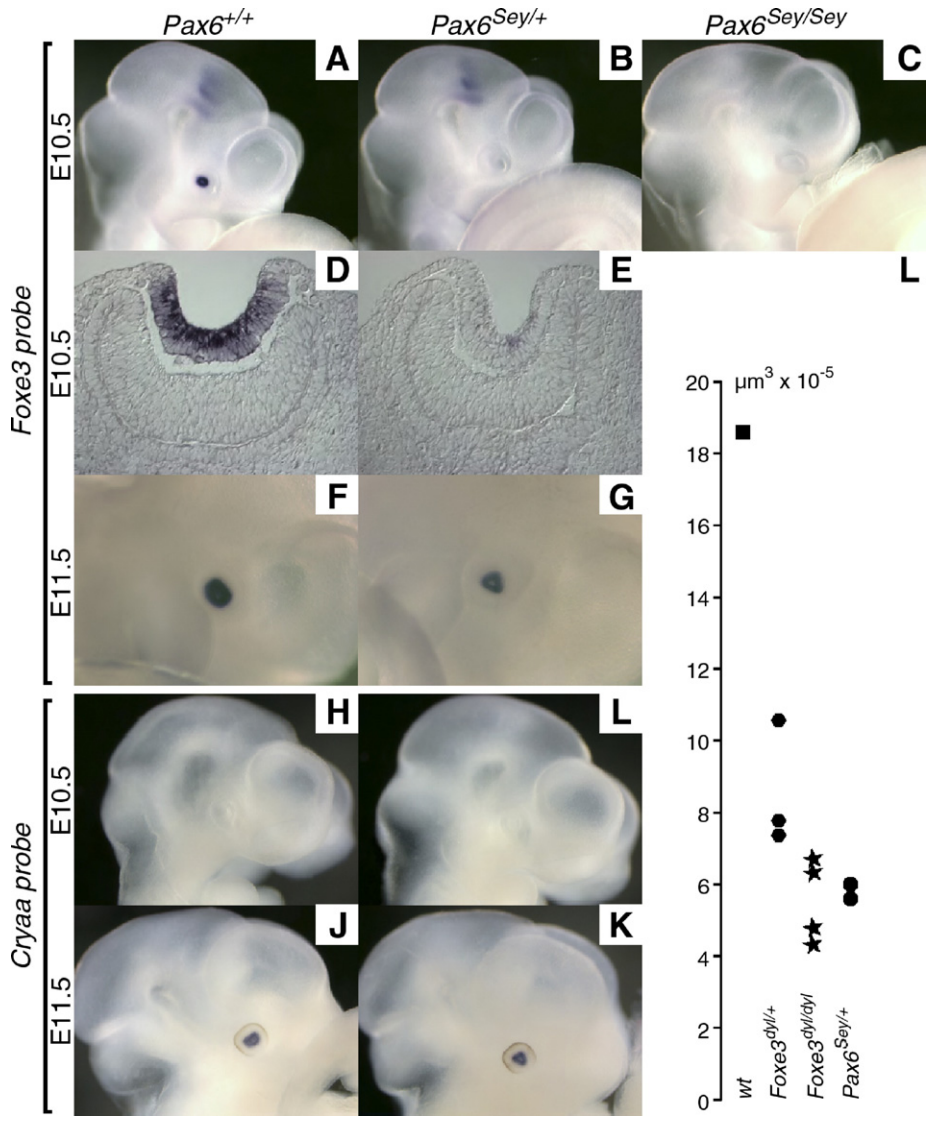

Fig. 6. Lens expression of *Foxe3* is sensitive to *Pax6* gene dosage. Whole mount (A–C; F–K) and section (D–E) *in situ* hybridization of E10.5 (A–E; H, I) and E11.5 (F, G, J, K) wild-type (A, D, F, H, J), $Pax6^{Sey/+}$ (B, E, G, I, K) and $Pax6^{Sey/Sey}$ (C) embryos with probes for *Foxe3* (A–G) and *Cryaa* (H–K). At E10.5 *Foxe3* is expressed in the lens pit and in a restricted area of the brain (A). Both areas of expression depend on *Pax6*, as seen by the absence of *Foxe3* expression in both brain and ocular surface ectoderm of $Pax6^{Sey/Sey}$ (C). However, the expression in the lens anlage differs from that of the brain in being highly sensitive to *Pax6* gene dosage; at E10.5 (A, B, D, E) there is a dramatic reduction in lens pit *Foxe3* mRNA of $Pax6^{Sey/+}$, compared to wild type, whereas the brain expression remains unaffected. At E11.5 (F, G) the difference is less pronounced, but still significant. In contrast, activation of a marker for lens differentiation, *Cryaa*, is synchronous in wild-type and *Pax6* mutant, and occurs around E11 (H–K). (L) Volume of lens pit tissue in E10.5 embryos (33 ± 1 somites) calculated from area measurements of serial sections. Wild-type: 1 eye; $Foxe3^{dyl/+}$: 3 eyes from two embryos; $Foxe3^{dyl/dyl}$: 4 eyes from two embryos; $Pax6^{Sey/+}$: two eyes from 1 embryo.

neurological or behavioral defects. However, since their behavior has not been thoroughly investigated, subtle defects may exist. The homozygous human subjects were reported to have no "cerebral malformations or dysmorphic features" and to "be in good health and have no intellectual or neurological impairment" (Valleix et al., 2006).

Is Pax6 haploinsufficiency a consequence of reduced Foxe3 expression?

Transcription of *Foxe3* in both lens and brain requires Pax6, as shown by the lack of expression in homozygous *Pax6* mutant embryos. *Pax6* is expressed in the surface ectoderm in the region where lens placode induction takes place and in the neuroectoderm of the optic vesicle that produces the inductive signal (Grindley et al., 1995; Walther and Gruss, 1991). As *Foxe3* transcription is activated in the surface ectoderm when lens placode formation is initiated (Blixt et al., 2000), the requirement for *Pax6* could be either direct—in the placode where both genes are co-expressed—or indirect, through signaling by the optic vesicle. Tissue recombination, chimerical embryos, targeted deletion of the Pax6 ectodermal enhancer and conditional knockout of Pax6 in the ectoderm, have convincingly demonstrated a cell

autonomous requirement for *Pax6* in the surface ectoderm for lens placode development, but showed it to be dispensable for the inductive capacity of the optic vesicle (Collinson et al., 2000; Davis-Silberman et al., 2005; Dimanlig et al., 2001; Fujiwara et al., 1994; Quinn et al., 1996). Hence, it is likely that Pax6 is needed in the pre-placode ectodermal cells for *Foxe3* expression. Consistent with this interpretation, targeted deletion of the *Pax6* ectodermal enhancer, which reduces placode but not optic cup expression, resulted in loss of *Foxe3* expression at E9.75 (Dimanlig et al., 2001).

Whether Pax6 activates the *Foxe3* promoter directly, or through other transcription factors is not known. Sequences upstream of the *Foxe3* coding region do contain putative Pax6 binding sites. However, functional assays *in vivo* will be required to settle this issue.

The most interesting aspect of the relation between *Pax6* and *Foxe3* is the gene dosage dependence. *Pax6* is essential for multiple events in CNS, eye and nasal development, but mainly anterior segment morphogenesis is disturbed when the null mutation is present in heterozygous form. In both mice and man, *Pax6* haploinsufficiency gives rise to variable defects in iris, lens and cornea (Baulmann et al., 2002; Davis et al., 2003; Glaser et al., 1994; Grindley et al., 1995; Hanson et al., 1994; Hill et al., 1991; Jordan et al., 1992; Ramaesh et al., 2003; Ton et al., 1991). The mechanism responsible for the requirement of two functional copies of *Pax6* is not known, but two models have been suggested. A critical step in development may require a threshold concentration of the Pax6 protein, for which expression from a single copy of the gene does not suffice. Alternatively, monoallelic expression—in combination with stochastic selection of the active allele and cell-autonomous requirement for the protein—would reduce the functional cell population by half. Nutt and Busslinger (1999) proposed monoallelic expression as a general explanation for haploinsufficiency of mammalian *Pax* genes, based on independent regulation of the two *Pax5* alleles during B cell development (Nutt et al., 1999). In the case of *Pax6*, however, this does not apply since biallelic expression has been demonstrated in the lens anlage of $Pax6^{Sey/+}$ embryos (van Raamsdonk and Tilghman, 2000).

The most plausible explanation is therefore that one or several target genes are highly sensitive to Pax6 concentration. This gene, or genes, would be predicted to be expressed in the developing lens, to be involved in anterior segment morphogenesis and to have a sensitive relationship between expression level and phenotype. *Foxe3* fulfils all these criteria. It is required in diploid dosage for normal eye development, its expression is sensitive to reduction in *Pax6* levels and the mutant phenotype consists of a spectrum of eye defects very similar to those of *Pax6* mutants. Independent confirmation of the sensitivity of the *Foxe3* promoter to *Pax6* gene dosage comes from a transgenic construct in which the *Foxe3* regulatory region drives the expression of *lacZ* (Brownell et al., 2000). The lens expression from this construct was reported to be "significantly reduced or absent" on $Pax^{Sey/+}$ background.

The main difference between $Pax6^{Sey/+}$ and $Foxe3^{-/+}$ phenotypes is the more severe iris hypoplasia in the *Pax6* mutant. Selective inactivation of one *Pax6* allele in either ectoderm or the distal optic cup showed that it is the ectodermal gene dosage that is important for all aspects of the *Sey* phenotype, except iris hypoplasia (Davis-Silberman et al., 2005). Iris size was more dependent on the optic cup gene dosage, although influenced also by the ectodermal expression level. Whereas reduced expression of *Foxe3* may explain all defects linked to halved ectodermal *Pax6* gene dosage, including a contribution to iris hypoplasia, the relevant Pax6 target gene(s) in the optic cup remain unknown.

$Pax6^{Sey/+}$ eyes are generally more seriously affected than those of $Foxe3^{-/+}$ heterozygotes, but not as severely as $Foxe3^{-/-}$ eyes. This would be consistent with the *Foxe3* mRNA level in $Pax6^{Sey/+}$ eyes being intermediary between that of $Foxe3^{-/+}$ and $Foxe3^{-/-}$ (with regard to functional mRNA, $Foxe3^{dyl/+}$ are expected to have approximately 50% of the wild-type amount since *Foxe3* is not autoregulated, Blixt et al., 2000).

$Pax6^{Sey/+}$ have smaller lenses and lens vesicles than normal littermates (Theiler et al., 1978). van Raamsdonk and Tilghman (2000) found this difference to be established at the time of lens pit invagination, prior to E10.5, and the growth rate of the lens after this event to be similar between wild-type and $Pax6^{Sey/+}$ embryos. This means that the reduction in lens size in $Pax6^{Sey/+}$ embryos is established when the deficit in *Foxe3* expression, compared to wild type, is greatest. The developing lenses of $Foxe3^{dyl/dyl}$ mutants are smaller than wild type (Blixt et al., 2000; Sanyal and Hawkins, 1979), and here we have shown that this difference exists already at E10.5 and that, to a lesser degree, it is evident also in *Foxe3* heterozygotes. This is consistent with a role for Foxe3 in lens placode and vesicle cell proliferation.

In conclusion, we propose that lowered expression of *Foxe3* is a major factor behind the defects observed in *Pax6* haploinsufficiency. Of course, this does not preclude contribution from other target genes with a similar response to alterations in Pax6 concentration, and in the case of iris hypoplasia, *Foxe3* is unlikely to be the main mediator.

Acknowledgments

We thank Helena Edlund for the *Sey* strain; The Swedish Medical Research Council (Vetenskapsrådet Medicin, grant #K2006-31X-13460-07-3) and The Swedish Cancer Foundation (Cancerfonden, grant #3517-B05-12XBC) for financial support.

References

Arffa, R.C., 1998. Grayson's Diseases of the Cornea. Mosby, St Louis.

Baulmann, D.C., Ohlmann, A., Flugel-Koch, C., Goswami, S., Cvekl, A., Tamm, E.R., 2002. Pax6 heterozygous eyes show defects in chamber angle differentiation that are associated with a wide spectrum of other anterior eye segment abnormalities. Mech. Dev. 118, 3–17.

Beebe, D.C., Coats, J.M., 2000. The lens organizes the anterior segment: specification of neural crest cell differentiation in the avian eye. Dev. Biol. 220, 424–431.

Blixt, Å., Mahlapuu, M., Aitola, M., Pelto-Huikko, M., Enerbäck, S., Carlsson, P., 2000. A forkhead gene, *FoxE3*, is essential for lens epithelial proliferation and closure of the lens vesicle. Genes Dev. 14, 245–254.

Brownell, I., Dirksen, M., Jamrich, M., 2000. Forkhead Foxe3 maps to the

dysgenetic lens locus and is critical in lens development and differentiation. Genesis 27, 81–93.
Collinson, J.M., Hill, R.E., West, J.D., 2000. Different roles for Pax6 in the optic vesicle and facial epithelium mediate early morphogenesis of the murine eye. Development 127, 945–956.
Davis, J., Duncan, M.K., Robison Jr., W.G., Piatigorsky, J., 2003. Requirement for Pax6 in corneal morphogenesis: a role in adhesion. J. Cell. Sci. 116, 2157–2167.
Davis-Silberman, N., Kalich, T., Oron-Karni, V., Marquardt, T., Kroeber, M., Tamm, E.R., Ashery-Padan, R., 2005. Genetic dissection of Pax6 dosage requirements in the developing mouse eye. Hum. Mol. Genet. 14, 2265–2276.
Dimanlig, P.V., Faber, S.C., Auerbach, W., Makarenkova, H.P., Lang, R.A., 2001. The upstream ectoderm enhancer in Pax6 has an important role in lens induction. Development 128, 4415–4424.
Fujiwara, M., Uchida, T., Osumi-Yamashita, N., Eto, K., 1994. Uchida rat (rSey): a new mutant rat with craniofacial abnormalities resembling those of the mouse Sey mutant. Differentiation 57, 31–38.
Gage, P.J., Rhoades, W., Prucka, S.K., Hjalt, T., 2005. Fate maps of neural crest and mesoderm in the mammalian eye. Investig. Ophthalmol. Vis. Sci. 46, 4200–4208.
Genis-Galvez, J.M., 1966. Role of the lens in the morphogenesis of the iris and cornea. Nature 210, 209–210.
Genis-Galvez, J.M., Santos-Gutierrez, L., Rios-Gonzalez, A., 1967. Causal factors in corneal development: an experimental analysis in the chick embryo. Exp. Eye Res. 6, 48–56.
Glaser, T., Jepeal, L., Edwards, J.G., Young, S.R., Favor, J., Maas, R.L., 1994. PAX6 gene dosage effect in a family with congenital cataracts, aniridia, anophthalmia and central nervous system defects. Nat. Genet. 7, 463–471.
Goudreau, G., Petrou, P., Reneker, L.W., Graw, J., Loster, J., Gruss, P., 2002. Mutually regulated expression of Pax6 and Six3 and its implications for the Pax6 haploinsufficient lens phenotype. Proc. Natl. Acad. Sci. U. S. A. 99, 8719–8724.
Grindley, J.C., Davidson, D.R., Hill, R.E., 1995. The role of Pax-6 in eye and nasal development. Development 121, 1433–1442.
Hanson, I.M., Fletcher, J.M., Jordan, T., Brown, A., Taylor, D., Adams, R.J., Punnett, H.H., van Heyningen, V., 1994. Mutations at the PAX6 locus are found in heterogeneous anterior segment malformations including Peters' anomaly. Nat. Genet. 6, 168–173.
Hill, R.E., Favor, J., Hogan, B.L., Ton, C.C., Saunders, G.F., Hanson, I.M., Prosser, J., Jordan, T., Hastie, N.D., van Heyningen, V., 1991. Mouse small eye results from mutations in a paired-like homeobox-containing gene [published erratum appears in Nature 1992 Feb 20;355(6362):750] Nature 354, 522–525.
Hogan, B.L., Horsburgh, G., Cohen, J., Hetherington, C.M., Fisher, G., Lyon, M.F., 1986. Small eyes (Sey): a homozygous lethal mutation on chromosome 2 which affects the differentiation of both lens and nasal placodes in the mouse. J. Embryol. Exp. Morphol. 97, 95–110.
Jordan, T., Hanson, I., Zaletayev, D., Hodgson, S., Prosser, J., Seawright, A., Hastie, N., van Heyningen, V., 1992. The human PAX6 gene is mutated in two patients with aniridia. Nat. Genet. 1, 328–332.
Kamachi, Y., Uchikawa, M., Tanouchi, A., Sekido, R., Kondoh, H., 2001. Pax6 and SOX2 form a co-DNA-binding partner complex that regulates initiation of lens development. Genes Dev. 15, 1272–1286.
Kidson, S.H., Kume, T., Deng, K., Winfrey, V., Hogan, B.L., 1999. The forkhead/winged-helix gene, Mf1, is necessary for the normal development of the cornea and formation of the anterior chamber in the mouse eye. Dev. Biol. 211, 306–322.
Lang, R.A., 2004. Pathways regulating lens induction in the mouse. Int. J. Dev. Biol. 48, 783–791.
Medina-Martinez, O., Brownell, I., Amaya-Manzanares, F., Hu, Q., Behringer, R.R., Jamrich, M., 2005. Severe defects in proliferation and differentiation of lens cells in Foxe3 null mice. Mol. Cell. Biol. 25, 8854–8863.
Nutt, S.L., Busslinger, M., 1999. Monoallelic expression of Pax5: a paradigm for the haploinsufficiency of mammalian Pax genes? Biol. Chem. 380, 601–611.
Nutt, S.L., Vambrie, S., Steinlein, P., Kozmik, Z., Rolink, A., Weith, A., Busslinger, M., 1999. Independent regulation of the two Pax5 alleles during B-cell development. Nat. Genet. 21, 390–395.
Ormestad, M., Blixt, Å., Churchill, A., Martinsson, T., Enerbäck, S., Carlsson, P., 2002. *Foxe3* haploinsufficiency in mice—A model for Peters' anomaly. Investig. Ophthalmol. Vis. Sci. 43, 1350–1357.
Quinn, J.C., West, J.D., Hill, R.E., 1996. Multiple functions for Pax6 in mouse eye and nasal development. Genes Dev. 10, 435–446.
Ramaesh, T., Collinson, J.M., Ramaesh, K., Kaufman, M.H., West, J.D., Dhillon, B., 2003. Corneal abnormalities in Pax6+/− small eye mice mimic human aniridia-related keratopathy. Investig. Ophthalmol. Vis. Sci. 44, 1871–1878.
Reneker, L.W., Silversides, D.W., Xu, L., Overbeek, P.A., 2000. Formation of corneal endothelium is essential for anterior segment development—A transgenic mouse model of anterior segment dysgenesis. Development 127, 533–542.
Sanyal, S., Hawkins, R.K., 1979. Dysgenetic lens (dyl)—A new gene in the mouse. Investig. Ophthalmol. Vis. Sci. 18, 642–645.
Semina, E.V., Brownell, I., Mintz-Hittner, H.A., Murray, J.C., Jamrich, M., 2001. Mutations in the human forkhead transcription factor FOXE3 associated with anterior segment ocular dysgenesis and cataracts. Hum. Mol. Genet. 10, 231–236.
Theiler, K., Varnum, D.S., Stevens, L.C., 1978. Development of Dickie's small eye, a mutation in the house mouse. Anat. Embryol. (Berl) 155, 81–86.
Ton, C.C., Hirvonen, H., Miwa, H., Weil, M.M., Monaghan, P., Jordan, T., van Heyningen, V., Hastie, N.D., Meijers-Heijboer, H., Drechsler, M., et al., 1991. Positional cloning and characterization of a paired box- and homeobox-containing gene from the aniridia region. Cell 67, 1059–1074.
Valleix, S., Niel, F., Nedelec, B., Algros, M.P., Schwartz, C., Delbosc, B., Delpech, M., Kantelip, B., 2006. Homozygous nonsense mutation in the FOXE3 gene as a cause of congenital primary aphakia in humans. Am. J. Hum. Genet. 79, 358–364.
Walther, C., Gruss, P., 1991. Pax-6, a murine paired box gene, is expressed in the developing CNS. Development 113, 1435–1449.
van Raamsdonk, C.D., Tilghman, S.M., 2000. Dosage requirement and allelic expression of PAX6 during lens placode formation. Development 127, 5439–5448.
Wigle, J.T., Chowdhury, K., Gruss, P., Oliver, G., 1999. Prox1 function is crucial for mouse lens-fibre elongation. Nat. Genet. 21, 318–322.
Yamada, R., Mizutani-Koseki, Y., Hasegawa, T., Osumi, N., Koseki, H., Takahashi, N., 2003. Cell-autonomous involvement of Mab21l1 is essential for lens placode development. Development 130, 1759–1770.
Zinn, K.M., 1970. Changes in corneal ultrastructure resulting from early lens removal in the developing chick embryo. Invest. Ophthalmol. 9, 165–182.